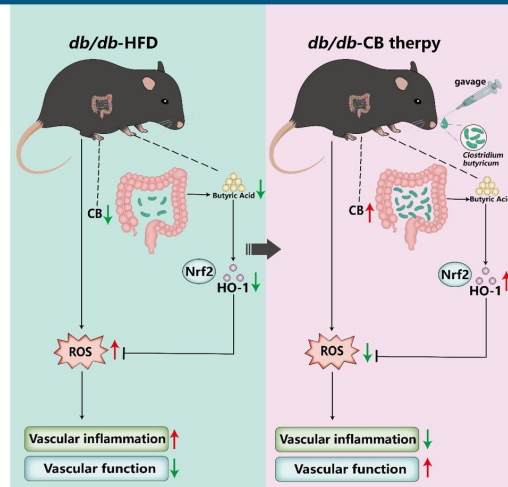


# Supplementation of *Clostridium butyricum* Alleviates Vascular Inflammation in Diabetic Mice

Tian Zhou, Shuo Qiu, Liang Zhang, Yangni Li, Jing Zhang, Donghua Shen, Ping Zhao, Lijun Yuan, Lianbi Zhao, Yunyou Duan, Changyang Xing

*Diabetes Metab J* 2024;48:390-404 | <https://doi.org/10.4093/dmj.2023.0109>

## Supplementation of *Clostridium butyricum* Alleviates Vascular Inflammation in Diabetic Mice



### Conclusion

This study identified the potential link between decreased CB abundance in gut microbiota and vascular inflammation in diabetes. Oral administration of CB alleviates the vascular lesions of diabetes mellitus by activating the Nrf2/HO-1 pathway.



### Highlights

- Hyperglycemic and high-fat diets decreased *Clostridium butyricum* (CB).
- Reduced butyrate levels led to diabetic vascular inflammation and dysfunction.
- Administering CB improved diabetic vascular lesion by activating Nrf2/HO-1 pathway.
- CB probiotics offer potential for protecting against diabetic vascular complications.

### How to cite this article:

Tian Zhou, Shuo Qiu, Liang Zhang, Yangni Li, Jing Zhang, Donghua Shen, Ping Zhao, Lijun Yuan, Lianbi Zhao, Yunyou Duan, Changyang Xing. Supplementation of *Clostridium butyricum* Alleviates Vascular Inflammation in Diabetic Mice. *Diabetes Metab J*. 2024;48:390-404. <https://doi.org/10.4093/dmj.2023.0109>



# Supplementation of *Clostridium butyricum* Alleviates Vascular Inflammation in Diabetic Mice

Tian Zhou<sup>1,\*</sup>, Shuo Qiu<sup>1,\*</sup>, Liang Zhang<sup>1,\*</sup>, Yangni Li<sup>2</sup>, Jing Zhang<sup>1,3</sup>, Donghua Shen<sup>4</sup>, Ping Zhao<sup>1</sup>, Lijun Yuan<sup>1</sup>, Lianbi Zhao<sup>1</sup>, Yunyou Duan<sup>1</sup>, Changyang Xing<sup>1,2</sup>

<sup>1</sup>Department of Ultrasound Diagnostics, Tangdu Hospital, Air Force Medical University, Xi'an, Departments of <sup>2</sup>Aerospace Medicine, <sup>3</sup>Biochemistry and Molecular Biology, Air Force Medical University, Xi'an, <sup>4</sup>Department of Ultrasound Diagnostics, The PLA Rocket Force Characteristic Medical Center, Beijing, China

**Background:** Gut microbiota is closely related to the occurrence and development of diabetes and affects the prognosis of diabetic complications, and the underlying mechanisms are only partially understood. We aimed to explore the possible link between the gut microbiota and vascular inflammation of diabetic mice.

**Methods:** The *db/db* diabetic and wild-type (WT) mice were used in this study. We profiled gut microbiota and examined the and vascular function in both *db/db* group and WT group. Gut microbiota was analyzed by 16s rRNA sequencing. Vascular function was examined by ultrasonographic hemodynamics and histological staining. *Clostridium butyricum* (CB) was orally administered to diabetic mice by intragastric gavage every 2 days for 2 consecutive months. Reactive oxygen species (ROS) and expression of nuclear factor erythroid-derived 2-related factor 2 (Nrf2) and heme oxygenase-1 (HO-1) were detected by fluorescence microscopy. The mRNA expression of inflammatory cytokines was tested by quantitative polymerase chain reaction.

**Results:** Compared with WT mice, CB abundance was significantly decreased in the gut of *db/db* mice, together with compromised vascular function and activated inflammation in the arterial tissue. Meanwhile, ROS in the vascular tissue of *db/db* mice was also significantly increased. Oral administration of CB restored the protective microbiota, and protected the vascular function in the *db/db* mice via activating the Nrf2/HO-1 pathway.

**Conclusion:** This study identified the potential link between decreased CB abundance in gut microbiota and vascular inflammation in diabetes. Therapeutic delivery of CB by gut transplantation alleviates the vascular lesions of diabetes mellitus by activating the Nrf2/HO-1 pathway.

**Keywords:** *Clostridium butyricum*; Diabetes mellitus; Gastrointestinal microbiome; NF-E2-related factor 2; Vascular diseases

## INTRODUCTION

Vasculopathy is one of the most common complications of diabetes mellitus (DM), which is also the main cause of casualties

in diabetic patients [1]. The hyperglycemia, insulin resistance and hyperinsulinemia are the main mechanisms of DM and progression to diabetic vascular complications [2,3]. In the conditions of hyperglycemia and insulin resistance, persistent

Corresponding authors: Changyang Xing <https://orcid.org/0000-0003-1605-8285>  
Department of Ultrasound Diagnostics, Tangdu Hospital, Air Force Medical University,  
Xinsi road No. 569th, Xi'an 710038, China  
E-mail: xingcy712@163.com

Yunyou Duan <https://orcid.org/0009-0008-6118-9018>  
Department of Ultrasound Diagnostics, Tangdu Hospital, Air Force Medical University,  
Xinsi road No. 569th, Xi'an 710038, China  
E-mail: duanyy@fmmu.edu.cn

Lianbi Zhao <https://orcid.org/0009-0008-7672-1759>  
Department of Ultrasound Diagnostics, Tangdu Hospital, Air Force Medical University,  
Xinsi road No. 569th, Xi'an 710038, China  
E-mail: libby0710@126.com

\*Tian Zhou, Shuo Qiu, and Liang Zhang contributed equally to this study as first authors.

Received: Apr. 12, 2023; Accepted: Jul. 10, 2023

This is an Open Access article distributed under the terms of the Creative Commons Attribution Non-Commercial License (<https://creativecommons.org/licenses/by-nc/4.0/>) which permits unrestricted non-commercial use, distribution, and reproduction in any medium, provided the original work is properly cited.

hyperglycemia leads to the formation of sugar-derived adducts referred as advanced glycation end-products (AGEs), which predisposes vessel walls to lipid deposition and triggers inflammatory responses [4]. AGEs are inducers of oxidative stress and inflammation through driving the production of reactive oxygen species (ROS) and free radicals, interrupting the secretion of nitric oxide, leading to endothelial dysfunction and ultimately accelerating the formation of atherosclerosis [5].

Currently, increasing evidence indicates that the pathogenesis of type 2 diabetes mellitus (T2DM) is closely related to the gut microbiota of the host in addition to obesity, genetic, and environmental factors [6]. The gut microbiota is referred as “microbial organs” in the human body, which participates in the body’s energy metabolism [7]. The gut microbiota is in a relatively upstream position in the progression of pre-diabetes, diabetes to diabetic complications, and mediates insulin resistance [8,9], oxidative stress [10] and chronic inflammation [11] mechanisms throughout the process. It is speculated that the intestinal microbiota may be closely related to the vascular complications of diabetes, and even the hyperglycemia and glucose variability in T2DM may be the result of gut microbiota imbalance [12-14]. However, the composition and function of the gut microbiota related with diabetic macroangiopathy have not been systematically studied, which may help us understand the occurrence and development diabetic vasculopathy complications, and contribute to the finding of new and early intervention targets.

In present study, we found that *Clostridium butyricum* (CB) and its metabolites were significantly reduced in the intestinal microbiota of diabetic mice, enhanced vascular oxidative stress and inflammatory response, and aggravated the damage of endothelial function. Therefore, *in vitro* and *in vivo* experiments were performed to evaluate the effects of CB intervention on vascular endothelial cells in mouse models of T2DM. In order to further explore the association between the intestinal microbiota and the vascular damage of T2DM, pulse wave velocity (PWV) was determined to evaluate the vascular stiffness by ultrasound. The anti-inflammatory and oxidative stress effects of CB were also investigated.

## METHODS

### Bacterial preparation

CB bio-53296 (ATCC19398, Beijing baioubowei Biotechnology Co. Ltd., Beijing, China) was grown on solid medium in agar-

supplemented reinforced clostridial medium (RCM) broth (Hopebio, Qingdao, China) for 48 hours in an anaerobic chamber (5% CO<sub>2</sub>) at 37°C, and cultured under RCM broth in anaerobic tubes sealed at 286 rpm at 37°C in an incubator shaker for 24 hours. Then, centrifuged and resuspended in sterile phosphate-buffered saline (PBS), and the final experimental concentration was 1.0×10<sup>10</sup> colony forming unit/kg per 2 days.

### Experimental animals and design

Male 5-week (Lepr) knockout (KO)/KO mice (*db/db*) and (Lepr) wild-type (WT)/WT mice purchased from GemPharmatech Limited Company (Nanjing, China) were fed in separate cages. Mice were maintained under standardized conditions at 20% humidity, and a temperature of 22°C to 24°C, and fed either a normal chow or high-fat diet with free access to water on a 12-hour light/12-hour dark cycle.

For CB treatment, the experimental group (diabetic [DB]-CB) mice were gavaged every 2 days with a suspension of CB (bio-53296, ATCC19398, Beijing Baioubowei Biotechnology Co. Ltd.) freshly prepared as previously described, once a day for 60 days. The DB-PBS group mice were gavaged with PBS instead. The WT mice were used as the control group. All mice at indicated time were subjected to PWV measurement as described below at the indicated times. At the end of the experiment, all animals were sacrificed and the tissues were isolated for further analysis. All animal experiments were carried out in accordance with the suspension guidelines of the Animal Care and Use Committee of Air Force Medical University (TD-201903-02).

### PWV measurement

Animal PWV was performed by experienced ultrasound technicians using Vevo 2100 imaging system (FUJIFILM VisualSonics, Toronto, ON, Canada). The mice were thoroughly depilated in advance, and were fixed with tape on the heated mouse plate with electrocardiogram connected. During pre-anesthesia, the inhalation concentration of isoflurane was 3% to 4%, and then maintained at 1.5% to 2.5% during the experiment. The Doppler velocity spectra were obtained at the ascending and abdominal aorta. PWV was calculated as the distance between abdominal aorta and ascending aorta signals detected divided by the time difference between two pulse arrivals relative to the R-wave of the electrocardiogram [15,16].

### Histology

At the end of the experiment, the aortic tissues of diabetic mice

were fixed in 4% paraformaldehyde for 24 hours, followed by embedding in paraffin sectioned at 10  $\mu\text{m}$  thickness. All cross sections were immediately stained with hematoxylin and eosin, Masson trichrome for histological analysis and observed via light microscopy.

### 16S rRNA sequencing and analysis

The abdominal cavity was exposed immediately after euthanasia, and the feces of each mouse (300 to 500 mg per mouse) were collected and stored immediately at  $-80^{\circ}\text{C}$ . The microbiota was analyzed by 16S rRNA sequencing as previously described [17] by Bioprofile (Shanghai, China). In brief, total DNA was extracted from feces, DNA was quantified by Nanodrop (Thermo Scientific, Waltham, MA, USA). Then, after quantitative polymerase chain reaction (qPCR) amplification of the sample target fragment, the library was quantified on the QuantiFluor (Promega, Madison, WI, USA) fluorescence quantitative system using the Quant-iT PicoGreen dsDNA Assay Kit. The processed sequences defined at a 97% similarity threshold were assigned to operational taxonomic units (OTUs). Sequence denoising or OTU clustering was performed according to the QIIME2 dada2 analysis procedure or the analysis procedure of Vsearch software (Open and Free Tool by Robert C. Edgar, USA).

### Short-chain fatty acids

Short-chain fatty acid (SCFA) composition was analyzed from fecal samples following the previously described protocol [18] by Bioprofile (Shanghai, China). Take 50 mg of sample, add 50  $\mu\text{L}$  15% phosphoric acid (Sinoreagent, Shanghai, China), add 125  $\mu\text{g}/\text{mL}$  internal standard (isocaproic acid, sigma, >98%) solution 100  $\mu\text{L}$  and diethyl ether (Sinoreagent) 400  $\mu\text{L}$  homogenize 1 minute, centrifuged at 12,000 rpm for 10 minutes at  $4^{\circ}\text{C}$ , and the supernatant was taken. Supernatants were analyzed by Thermo TRACE 1310-ISQ LT gas chromatography-mass spectrometry (GC-MS, Thermo Scientific).

### Immunofluorescence

Immunofluorescence was used to examine and quantify oxidant stress (via nuclear factor erythroid-derived 2-related factor 2 [Nrf2] and heme oxygenase-1 [HO-1]) in the arterial walls of diabetic mice. Arterial vascular tissue was collected and processed for paraffin embedding as previously described [19]. Paraffin sections were deparaffinized, serum blocked at room temperature, and incubated overnight at  $4^{\circ}\text{C}$  with anti-

Nrf2 (GB113808, Servicebio, Wuhan, China) and anti-HO-1 (GB12104, Servicebio), respectively, followed by fluorescence labeled secondary antibody. After these processes, the sections were counterstained with 4',6-diamidino-2-phenylindole (DAPI). All sections were visualized and images were captured with a fluorescent microscope (ECLIPSE C1, NIKON, Tokyo, Japan). Regions of interest positive for protein markers were selected from each image and measured via Image ProPlus 6.0 (Media cybernetics, Rockville, MD, USA).

### Measurement of reactive oxygen species

Superoxide levels were measured using the fluorescent dye dihydroethidium (DHE) (D7008, 1:500, Sigma, St. Louis, MO, USA) as previously described [20]. DHE, a cell-permeable fluorescent probe for assessing ROS levels, was oxidized by superoxide to ethidium bromide, which subsequently generates red fluorescence with DNA and was trapped within the nuclei of cells. Arterial vascular tissue was collected and processed for embedded in optimal cutting temperature compound at  $-80^{\circ}\text{C}$ . Tissue sections were incubated with DHE (2  $\mu\text{mol}/\text{L}$ ) at  $37^{\circ}\text{C}$  for 30 minutes. DHE oxidation products were extracted with acetonitrile. After the sections were washed three times, the images were observed and captured with a fluorescence microscope (ECLIPSE C1), and the fluorescence intensity was analyzed with Image ProPlus 6.0.

### Cell culture, high glucose, and butyrate treatment

Mouse aortic vascular smooth muscle cell (VSMC) line (MIC-iCell-c004 icell) was obtained from iCell Bioscience Inc., (Shanghai, China) and cultured in PriMed-iCELL-004 culture medium (iCell Bioscience Inc.) with 10% fetal bovine serum (FBS, Gemini, Life Technologies, Carlsbad, A, USA) and 1% antibiotic penicillin-streptomycin (Hyclone, Logan, UT, USA). Human umbilical vein endothelial cell (HUVEC) and RAW264.7 cell lines were obtained from American Type Culture Collection (ATCC, Manassas, VA, USA), cultured in Dulbecco's Modified Essential Medium (DMEM) culture medium (Hyclone) and RPMI 1640 Medium (Hyclone) respectively, both supplemented with 10% FBS and 1% antibiotic. The cultures were maintained in a humidified atmosphere containing 5%  $\text{CO}_2$  at  $37^{\circ}\text{C}$  until reaching 80% confluence and then passaged.

In order to investigate the effects of blood glucose on the vessels, all cells were stimulated with media with different sugar concentrations according to previous research methods [21,22].

After cells were passaged to passages 2–3, they were further incubated with normal glucose (NG; 5.5 mM) and high glucose (HG; 25 mM) for 24 hours. For butyrate treatment, in order to investigate the protective effect of sodium butyrate (SB) on the vascular endothelium, cells were cultured in HG (25 mM) for 24 hours, and then treated by addition of 5 mM SB (B5887, Sigma) for 24 hours, as previously described [23,24]. All experiments were repeated three times. Cells were collected for subsequent experiments.

### Western blot analysis

The protein samples from different groups of mouse aortic tissues were obtained by tissue grinding in radioimmunoprecipitation assay (RIPA) lysis buffer (Beyotime, Haimen, China). Protein concentrations were determined using bicinchoninic acid (BCA) Protein Assay Kit (Thermo Scientific). Then, the protein samples were separated via 10% or 12% sodium dodecyl sulfate-polyacrylamide gel electrophoresis (SDS-PAGE) and transferred onto polyvinylidene fluoride (PVDF) membranes (Immobilon P, Millipore, Burlington, MA, USA). Membranes were blocked with 8% milk in Tris-buffered saline containing 0.1% Tween-20 for 1 hour at room temperature. After blocking, membranes were incubated with Nrf2 (BF8017, Affinity Biosciences, Cincinnati, OH, USA) and HO-1 (AF5393, Affinity Biosciences) overnight at 4°C, followed by secondary antibodies for 1 hour at room temperature.  $\beta$ -Actin was used as an internal control. The bands were visualized using the enhanced chemiluminescent (ECL) Prime Western Blotting Detection Reagent (GE, Buckinghamshire, UK). Quantitative analysis of the Western blotting bands by ImageJ v1.8.0 software.

### qPCR analysis of the mRNA expression

The mRNA expression of interleukin 6 (IL-6), tumor necrosis factor- $\alpha$  (TNF- $\alpha$ ), Nrf2, and HO-1 was detected using real-time quantitative reverse transcription (RT-qPCR). Total RNA was extracted from all cells or mouse aortic tissues using the TRIzol (Invitrogen, Carlsbad, CA, USA) according to the manufacturer's instructions. Then, reverse transcription was done with the PrimeScript 1st Strand cDNA Synthesis Kit (Takara, Beijing, China). RT-qPCR analysis was performed using LightCycler Instrument 96 (Roche Diagnostic, Mannheim, Germany) and LightCycler Software 1.5 according to manufacturer's protocol. The relative mRNA expressions were calculated using  $2^{-\Delta\Delta Ct}$  method, and  $\beta$ -actin was used as the internal control.

### Statistical analysis

All data are expressed as the mean  $\pm$  standard error of the mean. Statistical significance was analyzed by GraphPad Prism 8.0 (GraphPad Software Inc., San Diego, CA, USA) using the Student's *t*-test for two group comparison or analysis of variance (ANOVA) for more than three groups. The between-group *post hoc* analyses were performed for the significant results of ANOVA analysis with Tukey's method. Differences with  $P < 0.05$  were considered statistically significant.

## RESULTS

### Aggravated vascular oxidative stress damage and arterial stiffness in the *db/db* mice

To investigate histological changes of vascular injury in macrovascular complications during diabetes progression of diabetes, we fed the *db/db* mice with a high-fat diet and the control group with a normal diet for 8 weeks, and the arterial stiffness was then assessed by PWV at day 1, 4, and 8 weeks of age (Fig. 1A and B). The aorta PWV in *db/db* mice showed a significant higher PWV in comparison with the control (Fig. 1C). All mice were euthanized at the end of the 8th week, and then tissues were taken for histological staining. The artery cross sections were stained with hematoxylin-eosin (HE) and Masson trichrome. In *db/db* mice, the vascular wall thickness was markedly increased, the smooth muscle fibers arrangement was disorderly, and the structure was blurred. Compared with the control group, vessels from *db/db* group mice exhibited an enlarged inter-smooth muscle cell space and subendothelial space filled with extracellular matrix and cellular debris. And quantitative analysis of Masson's staining revealed a significant increase in collagen deposition of *db/db* mice compared with control (Fig. 1D-F). Moreover, to detect ROS in the *ex vivo* aorta tissues of *db/db* and control mice, DHE staining was performed. The relative quantitative results showed that the fluorescence intensity of ROS signal in the *db/db* group was significantly stronger than that of the control group (Fig. 1G and H).

### Changes in gut microbiota in diabetic mice

The diversity of microbial communities was assessed using the alpha diversity index, which includes Chao1 index, Shannon index, and Faith's phylogenetic diversity (PD) index. Chao1 indices characterize richness, Shannon indices characterize diversity, and Faith's PD index characterize evolution-based diversity. The alpha diversity index of the *db/db* group was sig-

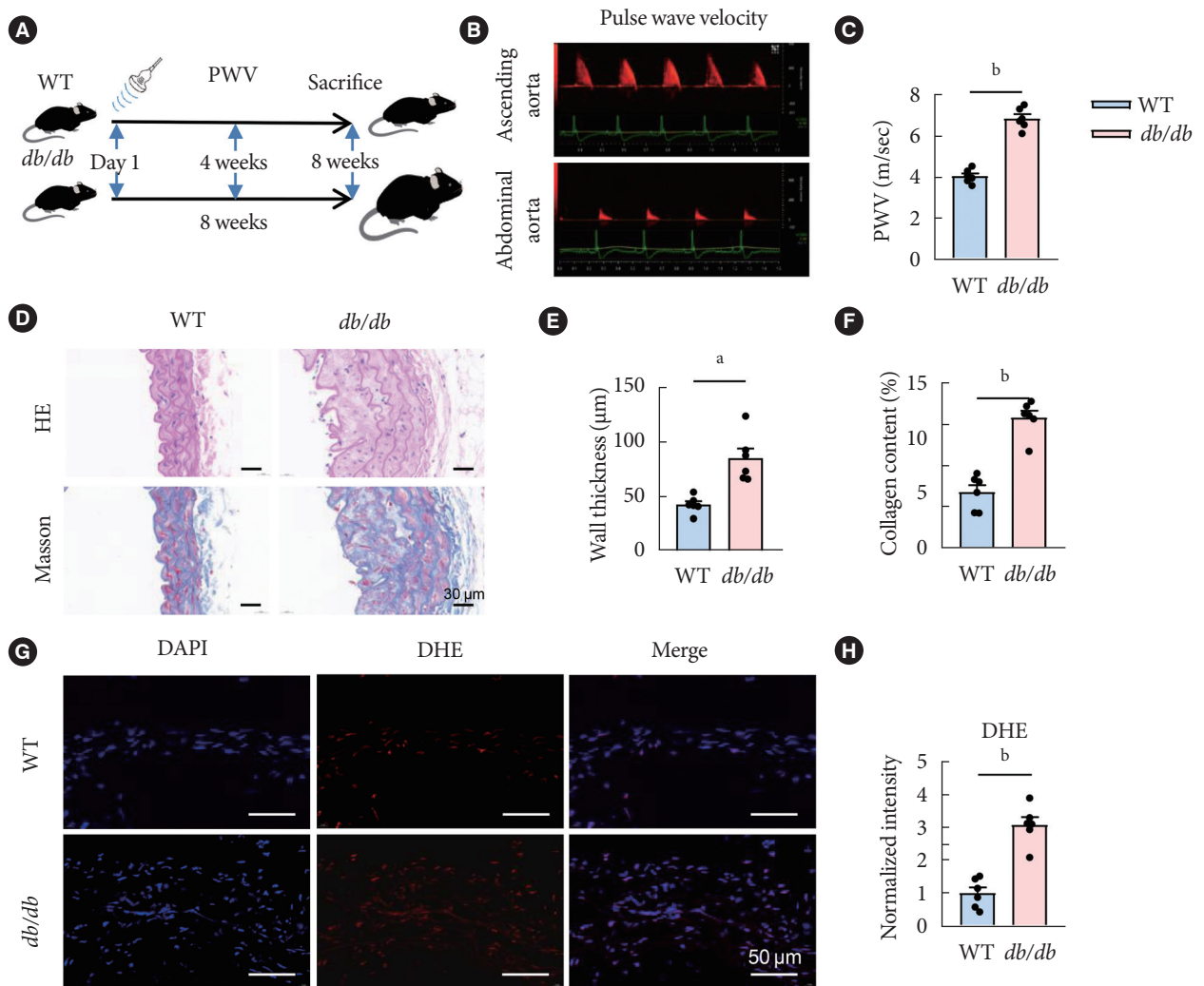


**Fig. 1.** The animal experiment procedure and vascular function change in the diabetic mice. (A) Schematic of experimental design. (B) Representative images of pulse wave velocity (PWV) measurement. PWV was determined at the ascending aorta and abdominal aorta, with the real-time electrocardiogram. (C) The PWV of the wild-type (WT) and *db/db* mice. (D) Hematoxylin/eosin (HE) and Masson's trichrome staining of blood vessels. Quantitative analysis of wall thickness (E) and collagen volume fraction (%) (F). (G) Fluorescence microscope images of the dihydroethidium (DHE) staining of the reactive oxygen species (red) in blood vessels of WT and *db/db* mice. Nuclei were counterstained with 4',6-diamidino-2-phenylindole (DAPI). All images at 80× magnification. (H) Quantification of the DHE fluorescence intensity by the software Image ProPlus 6.0 (Media cybernetics) in (D). Data were presented as mean ± standard error of the mean (*n* = 6 mice/group). A *t*-test was used for two independent groups. <sup>a</sup>*P* < 0.01, <sup>b</sup>*P* < 0.001.

nificantly lower than those in the control group (Fig. 2A). As seen from the principal component analysis, at the class and order level, the relative abundance of Clostridia and Clostridiales in *db/db* mice was significantly reduced as a proportion of the total species compared with WT mice (Fig. 2B and C). And the relative abundance of Clostridium\_vadinBB60\_group was also reduced as a proportion of the total species at the family and genus level in the fecal bacterial community of *db/db* mice

(Fig. 2D and E). In addition, at the level of class, order, family, and genus, the total OTUs of Clostridiales in the *db/db* mice were significantly decreased compared to WT mice (Fig. 2F).

**CB supplementation improves vascular function via gut microbiota remodeling and SCFAs change in diabetic mice**

To explore the potential effect of CB on vascular injury in diabetic mouse models, we administered 200 µL of CB suspension

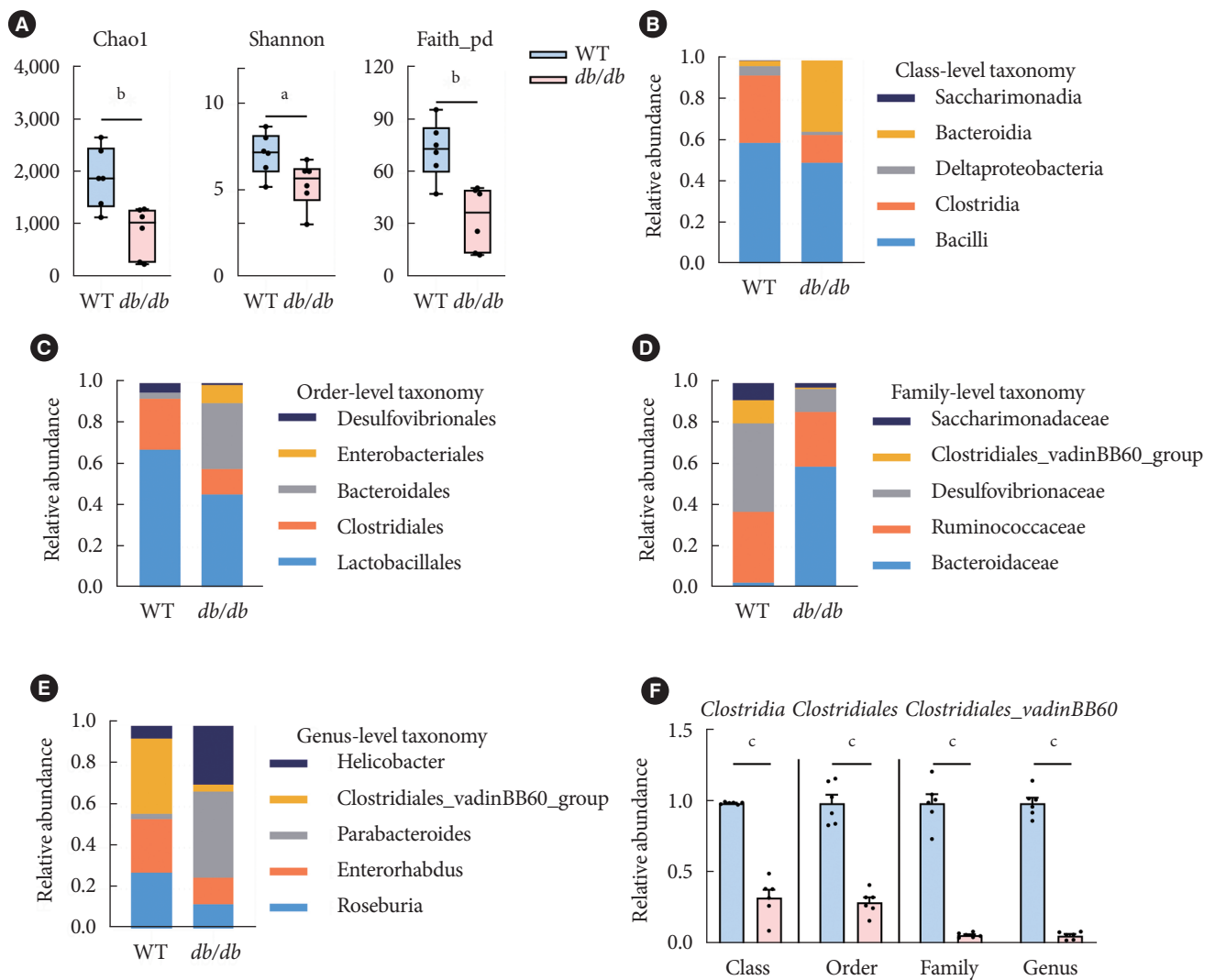
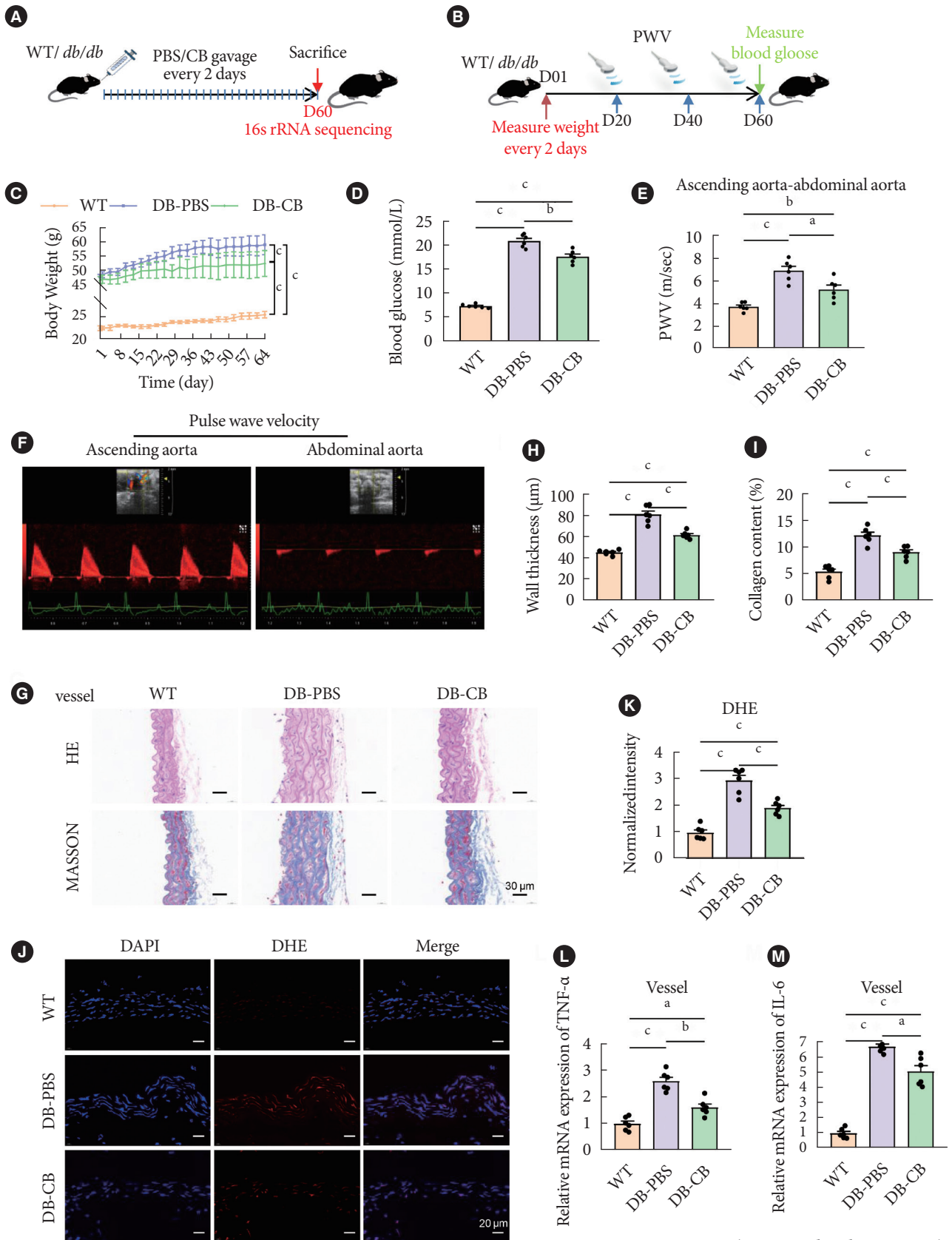


**Fig. 2.** Gut microbiota change in diabetic mice. (A) Alpha diversity was evaluated by Shannon, Chao1, and Faith-phylogenetic diversity (PD) indexes in gut flora. (B-E) Abundance of the main altered at classes (B), orders (C), families (D), and genera (E) levels in two groups, which displaying the decrease of Clostridia in *db/db* group. (F) The abundance of operational taxonomic units of Clostridia in the fecal bacterial community at classes, orders, families, and genera levels respectively in wild-type (WT) and *db/db* groups. Data were presented as mean  $\pm$  standard error of the mean ( $n=6$  mice/group). Analysis of variance followed by the indicated *post hoc* test was performed to determine the significance among the three groups. A *t*-test was used for two independent groups. <sup>a</sup> $P < 0.05$ , <sup>b</sup> $P < 0.01$ , <sup>c</sup> $P < 0.001$ .

every other day for 60 days (Fig. 3A). During this period, the body weight and the blood glucose level of the mice was measured. And vascular PWV detection was performed on mice on day 20, 40, and 60, respectively (Fig. 3B). Mice in the CB-treated group gained weight significantly slower than the *db/db* mice in the PBS-treated group (Fig. 3C). After the treatment with CB, the blood glucose level was significantly decreased compared with DB-PBS group (Fig. 3D). The aorta

PWVs were different across the groups, which suggested alterations in vascular stiffness. PWVs were significantly increased in untreated DB-PBS group mice compared to age-matched WT mice, and CB-treated DB mice have significantly lower PWV than non-treated DB mice. The mean PWVs in WT, DB-CB, and DB-PBS group was 3.69, 5.22, and 6.88 m/sec, respectively. The CB-treated DB mice group decreased the PWV value by 24.21% (Fig. 3E and F).



(Continued to the next page)



**Fig. 3.** Supplementation of *Clostridium butyricum* (CB) alleviates vascular phenotype, inflammation and oxidative stress in diabetic mice. (A, B) Schematic representation of the experimental procedure. (C) Weight change of every group. (D) Blood glucose change of every group. (E) The pulse wave velocity (PWV) of the wild-type (WT), diabetic (DB)-phosphate-buffered saline (PBS) and DB-CB group at ascending aorta to abdominal aorta. (F) Ultrasound representative images of PWV. (G) Vascular change as revealed by Hematoxylin/eosin (HE) and Masson's trichrome staining. (H) Wall thickness, (I) collagen volume fraction (%) of the arteries of mice receiving CB treatment for 60 days. (J) Fluorescence microscope images of the dihydroethidium (DHE) staining of the reactive oxygen species (red) in arterial tissue of three groups mice. Nuclei were counterstained with 4',6-diamidino-2-phenylindole (DAPI). All images at 80× magnification. (K) Quantification of DHE fluorescence intensity by the software Image Pro-Plus 6.0 (Media cybernetics). (L, M) Real-time quantitative reverse transcription analysis of the mRNA expression of the inflammatory cytokines interleukin 6 (IL-6) and tumor necrosis factor- $\alpha$  (TNF- $\alpha$ ) in arterial tissue of three groups. Data were presented as mean  $\pm$  standard error of the mean ( $n=6$  mice/group). Analysis of variance followed by the indicated *post hoc* test was performed to determine the significance among the three groups. <sup>a</sup> $P<0.05$ , <sup>b</sup> $P<0.01$ , <sup>c</sup> $P<0.001$ . (Continued)

We next explored whether CB supplementation would be beneficial to prevent inflammatory changes in blood vessels in diabetic mice; All mice were euthanized at day 60, and then tissues were taken for histological staining. HE staining showed that the vascular wall thickness was markedly increased in diabetic mice; however, compared with the DB-PBS group, it was significantly decreased after oral gavage of CB in DB-CB group ( $P<0.01$ ) (Fig. 3G and H). Consistently, there was increased collagen deposition in vascular wall in DB-PBS mice group as revealed by Masson's trichrome staining. And in the DB-CB group, there was a significant improvement in smooth muscle fiber sparseness, disorder, and collagen deposition compared with the DB-PBS group ( $P<0.01$ ) (Fig. 3G and I). To detect ROS in the aorta tissues of *db/db* and WT mice, DHE staining was performed. The results showed that the fluorescence intensity of the ROS signal in the DB-PBS group was significantly stronger than that in the WT group, while the diabetic group treated with CB was significantly lower than the DB-PBS group ( $n=6$ ,  $P<0.01$ ) (Fig. 3J and K). After 60 days, the inflammatory response was improved, and the qPCR of arterial tissue results showed that the mRNA expression of inflammatory cytokines (IL-6 and TNF- $\alpha$ ) were found to be significantly reduced in DB-CB group mice after CB treatment compared with those in the untreated DB-PBS group mice ( $n=6$ ,  $P<0.01$ ) (Fig. 3L and M).

To investigate changes in gut microbiota after microbiota transplantation of CB gavage in diabetic mice, the gut microbiota was analyzed by 16sRNA sequencing in 60-day CB gavage-treated *db/db* mice and control mice (Fig. 3A). The diversity of the microbial community significantly decreased in the DB-PBS group, while the microbial community diversity of the DB-CB group was not significantly different from the WT group (Fig. 4A). Beta diversity also significantly differed between habitat types (Fig. 4B). We constructed a Venn diagram

to determine the degree of OTU overlap between samples, which showed that the overlap between the DB-CB group and the WT group was 2.29%, and the overlap between the DB-PBS group and the WT group was 1.61% (Fig. 4C). Linear discriminant analysis (LDA) effect size (LEfSe) analysis indicating significant differences in bacterial taxa (LDA score  $>2.0$ ; alpha value  $P<0.05$ ). At the genus level, LEfSe analysis identified LDA scores above 2.0 for each group of genera. LEfSe identified genera that were differentially enriched in OTUs between the DB-PBS group and the other two groups, such as: Clostridiales\_vadinBB60\_group (increased in WT group; LDA score = 3.23,  $P=0.025$ ; increased in DB-CB group; LDA score = 2.98,  $P=0.040$ ). In addition, Clostridiales\_vadinBB60\_group were significantly deficient in DB-PBS group (Fig. 4D). At the level of order and family taxonomy, the total OTUs of Clostridiales in DB-CB group were significantly increased compared to DB-PBS group, which was not gavaged with CB (Fig. 4E and F). A notable decrease in butyric acid content in diabetic mice feces compared to WT group, while treated with CB by oral gavage (DB-CB group) showed increased levels ( $P<0.01$ ) of butyric acid in comparison with DB-PBS group (Fig. 4G).

### The function of CB supplementation correlates with Nrf2 and HO-1 restoration

Studies have confirmed that oxidative stress would be inhibited through activation the Nrf2/HO-1 signaling pathway. To further explored the relationship between CB intestinal intervention and oxidative stress in diabetic mice, we performed immunofluorescence staining and Western blot quantitative detection the level of Nrf2 and HO-1 proteins in vascular tissues of the mice model. The results showed that the fluorescence intensity of Nrf2 and HO-1 signals both in DB-CB group and DB-PBS group was significantly stronger than that in WT group.

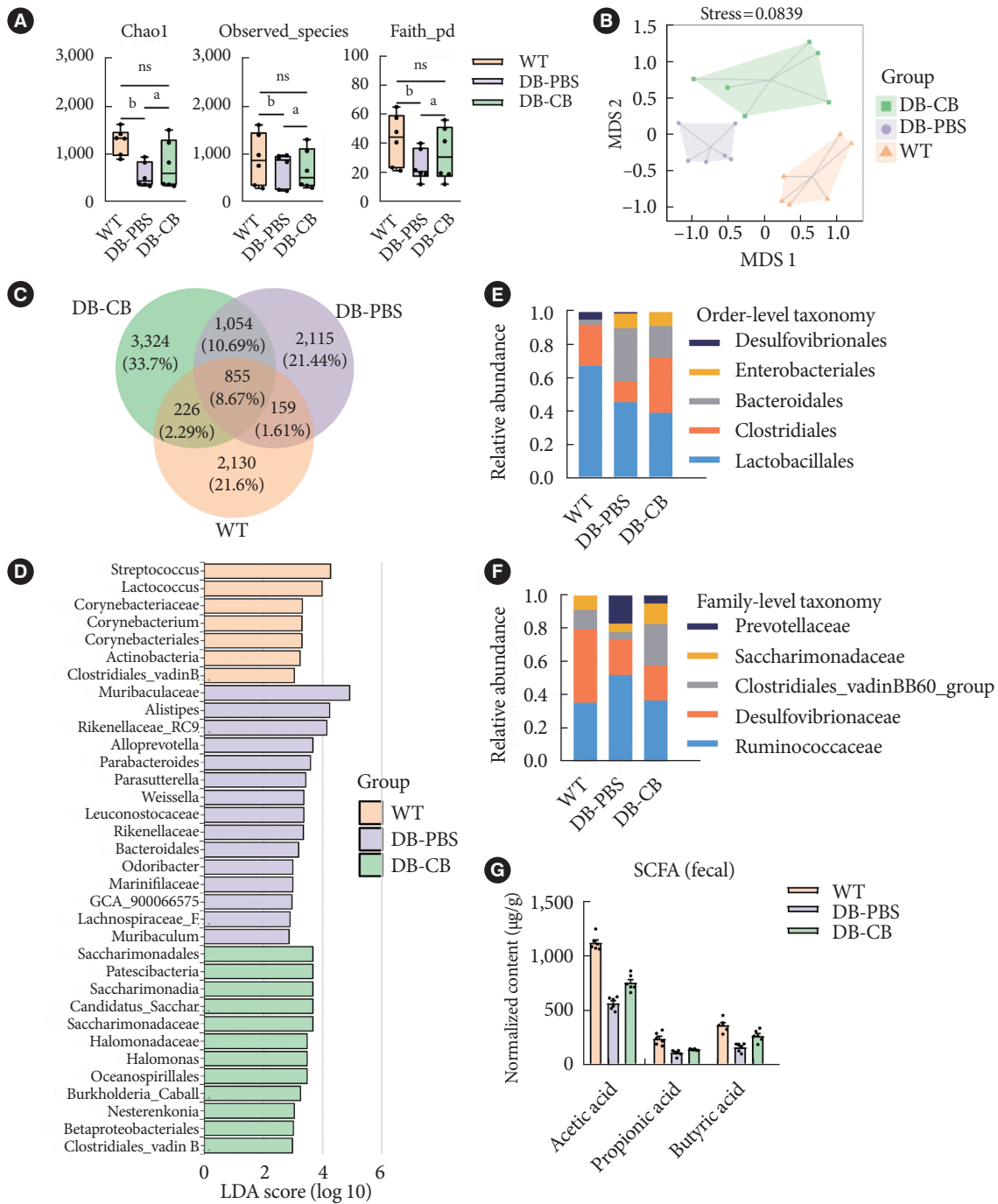


**Fig. 4.** *Clostridium butyricum* (CB) supplementation increases the metabolite butyrate in diabetic mice. (A) Alpha diversity was evaluated by Shannon, Chao1 and Faith-phylogenetic diversity (PD) indexes in gut flora. (B) Beta diversity of gut microbiota in three groups. (C) Venn diagram illustrates the overlap of operational taxonomic units in gut microbiota among three groups. (D) Linear discriminant analysis (LDA) effect size (LEfSe) identifies the taxa with the greatest differences in the abundance among three groups. Only the taxa with meeting a significant LDA threshold value of >2 were shown. Comparisons of the relative abundance of Clostridia in the fecal bacterial community at (E) bacterial order (orange), and (F) family (grey) levels. (G) The level of butyrate in the fecal samples. Data were presented as mean ± standard error of the mean ( $n=6$  mice/group). Analysis of variance followed by the indicated *post hoc* test was performed to determine the significance among the three groups. WT, wild-type; DB, diabetic; PBS, phosphate-buffered saline; ns, no significance; SCFA, short-chain fatty acid. <sup>a</sup> $P < 0.05$ , <sup>b</sup> $P < 0.01$ .

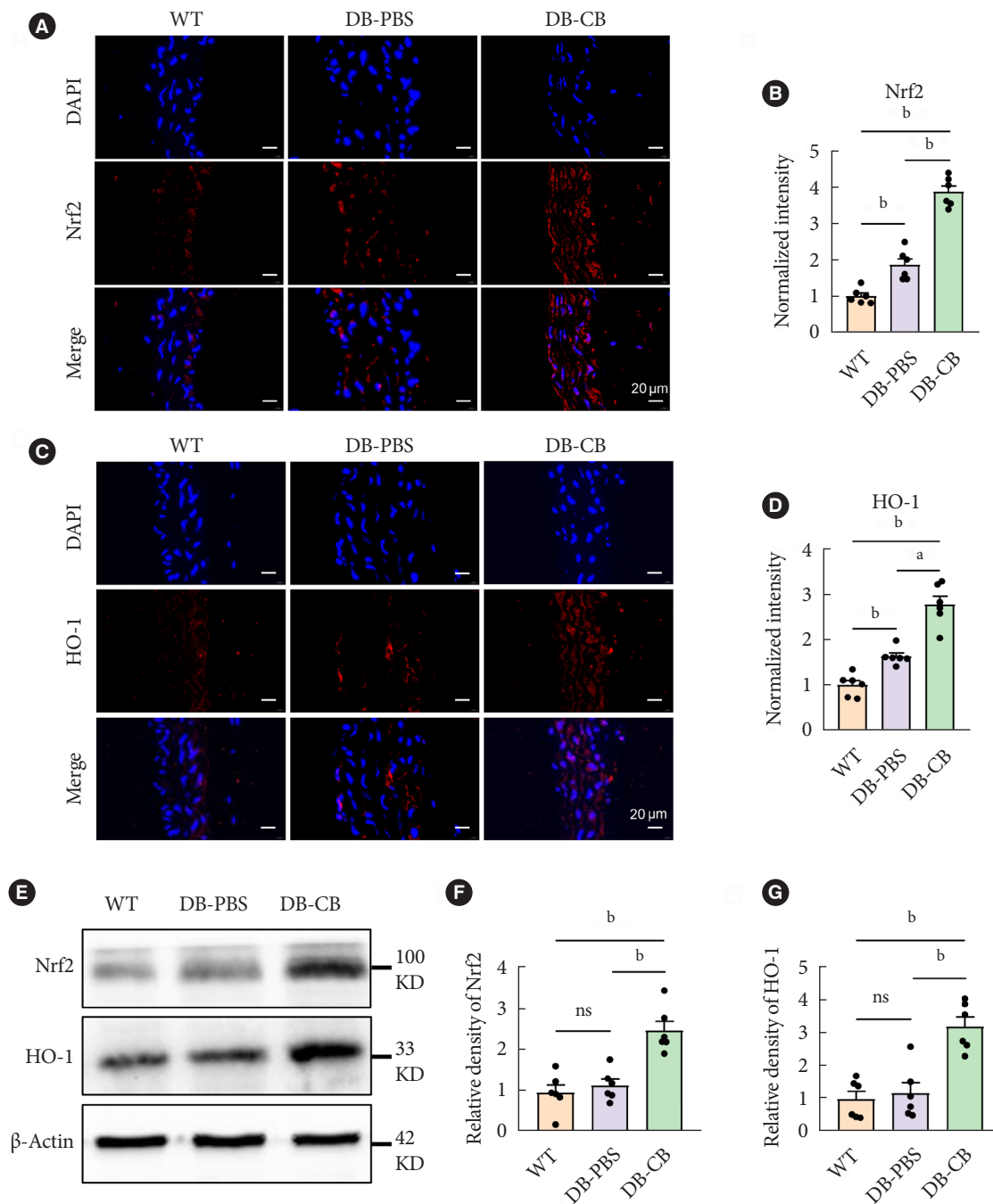


**Fig. 5.** Oral administration of *Clostridium butyricum* (CB) increases the expression levels of nuclear factor erythroid-derived 2-related factor 2 (Nrf2) and heme oxygenase-1 (HO-1) in arteries of diabetic mice. (A, C) Immunofluorescence analysis using an antibody against Nrf2 and HO-1 on vascular histological sections prepared from animals orally administered CB. Images were acquired at 80× magnification (red=Nrf2 and HO-1; blue=4',6'-diamidino-2-phenylindole [DAPI]). (B, D) Quantification of the Nrf2 and HO-1 fluorescence intensity by the software Image ProPlus 6.0 (Media cybernetics). (E) The protein level of Nrf2 and HO-1 in arterial tissue of three groups mice was determined by Western blotting. Representative data of at least three independent experiments. (F, G) Quantification of relative density of the Nrf2 and HO-1 Western blotting bands by the software ImageJ v1.8.0. Data were presented as mean ± standard error of the mean ( $n=6$  mice/group). Analysis of variance followed by the indicated *post hoc* test was performed to determine the significance among the three groups. WT, wild-type; DB, diabetic; PBS, phosphate-buffered saline; KD, kilodalton; ns, no significance. <sup>a</sup> $P<0.01$ , <sup>b</sup> $P<0.001$ .

However, the fluorescence intensity of Nrf2 and HO-1 signals in DB-PBS group was significantly weaker than that in DB-CB group with CB-treated ( $n=6, P<0.01$ ) (Fig. 5A-D). Moreover, representative Western blot results and relative quantitation of

Western blot are shown that the increased levels of Nrf2 and HO-1 proteins in the DB-CB group compared with the DB-PBS group ( $n=6, P<0.05$ ) (Fig. 5E-G).

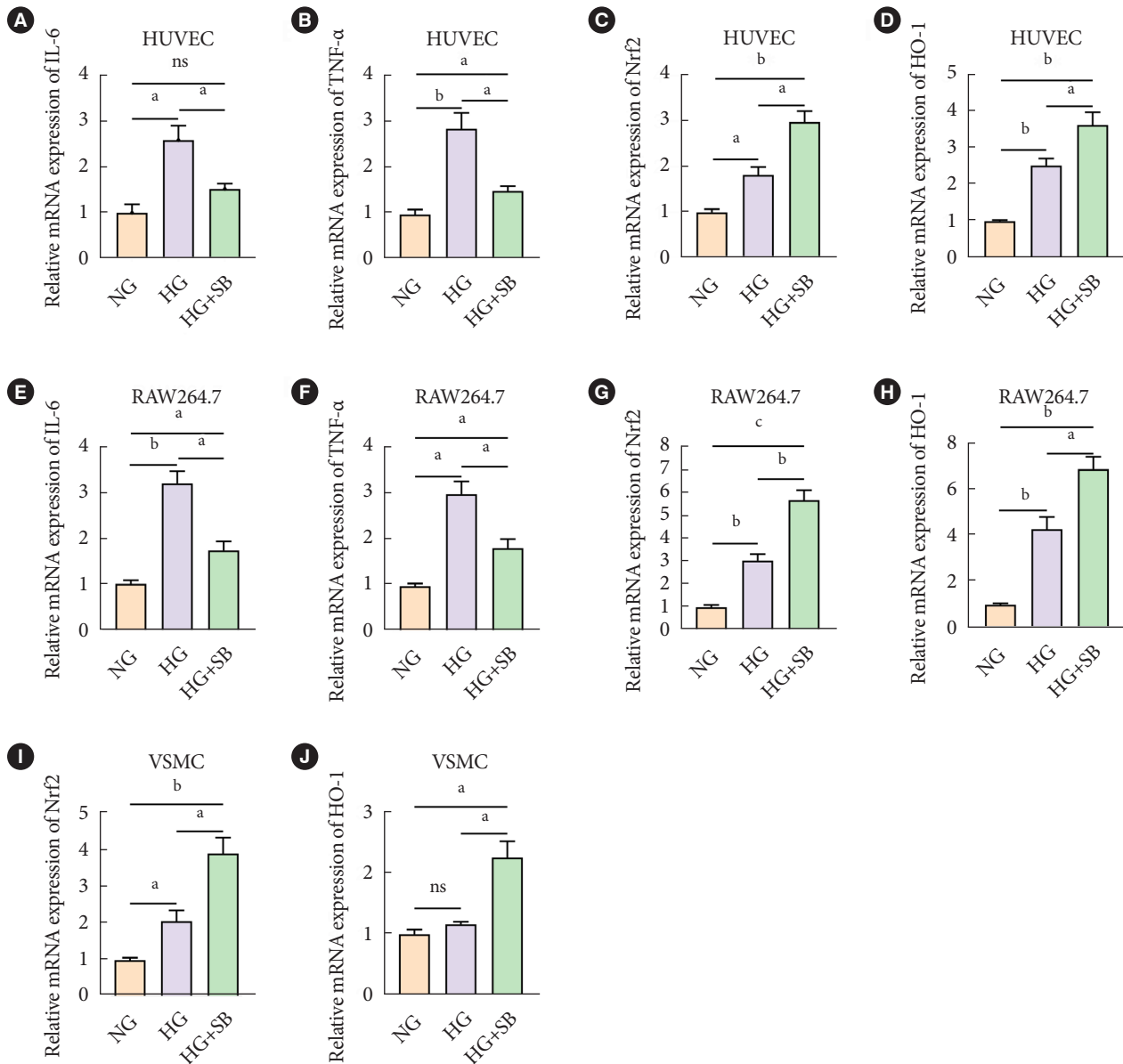


**Fig. 6.** Sodium butyrate (SB) inhibits high glucose (HG)-induced cellular inflammation and oxidative stress in multiple cells. (A, B, E, F) The expression level of the inflammatory cytokines interleukin 6 (IL-6) and tumor necrosis factor- $\alpha$  (TNF- $\alpha$ ) mRNA was analyzed by quantitative polymerase chain reaction (qPCR), in HG-induced human umbilical vein endothelial cell (HUVEC) and RAW264.7 cells respectively. (C, D, G-J) The mRNA expression level of nuclear factor erythroid-derived 2-related factor 2 (Nrf2) and heme oxygenase-1 (HO-1) was analyzed by qPCR, in HG-induced all groups. Data were presented as mean  $\pm$  standard error of the mean of three biological replicates. Analysis of variance followed by the indicated *post hoc* test was performed to determine the significance among the three groups. NG, normal glucose; ns, no significance; VSMC, vascular smooth muscle cell. <sup>a</sup> $P<0.05$ , <sup>b</sup> $P<0.01$ , <sup>c</sup> $P<0.001$ .

### SB represses the inflammatory reactions caused by HG, and elevates the levels of Nrf2 and HO-1

It is generally believed that inflammation play pivotal role in the progression of diabetic vascular complications [25]. Therefore, we investigated the effects of SB on inflammatory cytokines in HUVEC, RAW264.7 and VSMC cells. RT-qPCR results showed that in HUVEC and RAW264.7 cells experiments respectively, the mRNA expression levels of IL-6 and TNF- $\alpha$  in HG group were significantly higher than those in NG group, whereas the HG+SB group treated with SB significantly decreased the mRNA expression levels of IL-6 and TNF- $\alpha$  ( $P < 0.05$ ) (Fig. 6A, B, E, and F). Moreover, in HUVEC, RAW264.7 and VSMC cell experiments, compared with NG group, the mRNA expression levels of Nrf2 and HO-1 both in HG group and HG+SB group were significantly increased. And the mRNA expression levels of Nrf2 and HO-1 in HG+SB group were significantly higher than those in HG group ( $P < 0.05$ ) (Fig. 6C, D, and G-J).

## DISCUSSION

Vasculopathy is a severe complication of diabetes due to uncontrolled HG, and a major cause of morbidity and mortality [1]. It has been reported that fecal microbiota transplantation is an effective treatment for T2DM by reverse insulin resistance and islet damage [26]. However, whether there is a potential link between the gut microbiota and vascular complications in diabetic patients is yet to be clarified. Therefore, to explore the relationship between the gut microbiota and vascular complications of diabetes, using a *db/db* mouse model, we demonstrated inflammatory and oxidative stress damage in diabetic vessels. It was further revealed that the alteration of gut microbiota, especially the reduction of butyric acid bacteria, might be responsible for the vascular inflammation and oxidative stress in diabetic mice. Oral supplementation of CB partially retarded weight gain, vascular dysfunction and oxidative stress in diabetic mice. Our findings, for the first time, indicate that CB may attenuate vascular inflammatory and oxidative stress of DM effectively via activating the Nrf2/HO-1 pathway. Regulation of gut microbiota could be helpful for the management of diabetic vascular complications.

An increasing number of studies have confirmed that excessive inflammatory response and oxidative stress often occur in the progression of hyperglycemia and insulin resistance-induced metabolic disorders [27]. Theoretically, persistent hyperglycemia can cause the vascular wall to more easily “cap-

ture” lipids, leading to disorders of glucose and lipid metabolism, promoting the production of ROS and free radicals, triggering oxidative stress and inflammatory responses, and aggravating vascular endothelial dysfunction [28]. In this study, using diabetic mouse model fed with a high-fat diet, we confirmed that diabetic mice had severe vascular inflammation and oxidative stress damage, and further found that altered in intestinal flora of diabetic mice, especially decreased CB.

Studies have shown that the composition and function of the gut microbiota play a crucial role in obesity and metabolic disease [29]. The microbial metabolites, SCFAs, are the “secret weapons” of intestinal bacteria. Butyric acid, acetic acid, and propionic acid are all involved in the regulation of energy metabolism. Moreover, several effective T2DM therapies, such as metformin and berberine, have been reported to be able to restore the abundance of SCFA-producing bacteria [30]. CB is one of the main sources of butyric acid. In a mouse model of obesity, oral butyrate reduces food intake by stimulating the vagus nerve to induce a constant feeling of satiety [31]. It has also been shown that hypoglycemic effects are achieved by increasing the number of butyrate-producing bacteria in the gut of a T2DM mouse model, resulting in the production of butyrate and the secretion of glucagon-like peptide-1 and insulin [32]. CB played an important role in diabetic vasculopathy not only through butyrate, but also through immune and other mechanisms. CB interacts with a variety of systemic immune cells to influence systemic inflammation [33,34], which then influences the development of vascular complications involved in diabetes. Thus, *in vivo* experiments, our study confirmed that the intestinal CB in the diabetic mouse model was reduced compared with normal mice. Intragastrically transplanted CB significantly reduced blood glucose, delayed weight gain, and improved vascular inflammation and oxidative stress in diabetic mice. In addition, other than the CB strain used in present study (ATCC19398), the CB CGMCC0313.1 may also be a promising CB strain in the protection for diabetic vascular injury duo to its therapeutic benefit in improving metabolic diseases reported previously [35,36]. The gene and function differences between these two strains worths further investigations.

Oxidative stress has an important role in the pathogenesis of diabetes and its complications [37,38]. Nrf2 is a redox-sensitive transcription factor that is generally silent [39]. Activation of the Nrf2 signaling pathway can induce upregulation of antioxidant enzyme gene expression and thus protect organs damaged by oxidative stress induced by hyperglycemia in diabetes

[40]. And the activation of Nrf2 signaling ameliorates DM by protecting pancreatic beta cells and suppressing gluconeogenesis-related gene expression [41], suggesting that the Nrf2 system is a critical target for preventing the onset of DM. Additionally, activated Nrf2 enters the cell nucleus and exerts antioxidant effects through its interaction with downstream antioxidant genes such as HO-1 [42]. According to the aforementioned results, the high fasting blood glucose levels in diabetic rats were significantly reduced upon oral administration of CB. Therefore, it is confirmed by present study that CB treatment activates the Nrf2 system by increasing the level of butyrate in the blood, thus achieving a reduction in the ROS content of arteries, decreasing vascular oxidative stress and improving vascular function. To further explore the mechanism, using an experimental model of HG-induced HUVEC, RAW264.7 and VSMC cells, it was found that the elevation of inflammatory cytokine levels by HG were significantly reduced after SB treatment. And SB treatment also increased the levels of Nrf2 and HO-1 in HUVEC, RAW264.7 and VSMC cells. Based on the above results, we speculate that the mechanism of SB in regulating oxidative damage during the development of diabetic vascular complications may be related to the Nrf2/HO-1 pathway. However, our study found that CB intervention acted on diabetic vasculopathy not only by increasing butyrate in the blood, but also by improving the diversity of the intestinal flora, increasing the content of probiotic bacteria in the intestinal flora, improving the disordered intestinal flora in diabetic mice, and eventually stopping the progression of diabetic vascular complications. Moreover, the genes and receptor mRNA expression could significantly influence the effects of butyrate. Multiple genes and receptors, and their complex interactions could all involved in the functioning of butyrate as shown by previous studies [35,36]. Metagenome sequencing may help answer this question.

In this study, we first found the association between microbiota and diabetes vascular complications, and further developed the corresponding therapeutic strategy by microbiota transplantation. The supplementation of CB could increase the metabolite butyrate levels, regulate gut microbiota diversity, and thus reduce the blood glucose, decelerate weight gain and improve the vascular function through the alleviation of vascular inflammatory and oxidative stress by Nrf2/HO-1 pathway in diabetic mice. It would be of great clinical interest to explore complementary reagents of CB probiotics for diabetes vascular protection.

## CONFLICTS OF INTEREST

No potential conflict of interest relevant to this article was reported.

## AUTHOR CONTRIBUTIONS

Conception or design: T.Z., L.Z., Y.D., C.X.

Acquisition, analysis, or interpretation of data: all authors.

Drafting the work or revising: T.Z., S.Q., Y.D., C.X.

Final approval of the manuscript: all authors.

## ORCID

Tian Zhou <https://orcid.org/0000-0002-7690-1206>

Shuo Qiu <https://orcid.org/0009-0008-4804-8640>

Liang Zhang <https://orcid.org/0009-0007-1973-1865>

Lianbi Zhao <https://orcid.org/0009-0008-7672-1759>

Yunyou Duan <https://orcid.org/0009-0008-6118-9018>

Changyang Xing <https://orcid.org/0000-0003-1605-8285>

## FUNDING

This study was supported by grants from National Natural Science Foundation of China (No. 81901751 and 81901861) and Innovative Talent Promotion Program of Shaanxi Province (2022KJXX-106). Changyang Xing was also supported by the Special Fund for Aerospace Medical Research.

## ACKNOWLEDGMENTS

We are grateful for the technical help from Guodong Yang. We would also express our thanks for all the lab members for critical reading of the manuscript.

## REFERENCES

1. Pearson-Stuttard J, Cheng YJ, Bennett J, Vamos EP, Zhou B, Valabhji J, et al. Trends in leading causes of hospitalisation of adults with diabetes in England from 2003 to 2018: an epidemiological analysis of linked primary care records. *Lancet Diabetes Endocrinol* 2022;10:46-57.
2. Laakso M, Kuusisto J. Insulin resistance and hyperglycaemia in cardiovascular disease development. *Nat Rev Endocrinol* 2014; 10:293-302.

3. Paneni F, Costantino S, Cosentino F. Insulin resistance, diabetes, and cardiovascular risk. *Curr Atheroscler Rep* 2014;16:419.
4. Hill MA, Yang Y, Zhang L, Sun Z, Jia G, Parrish AR, et al. Insulin resistance, cardiovascular stiffening and cardiovascular disease. *Metabolism* 2021;119:154766.
5. James DE, Stockli J, Birnbaum MJ. The aetiology and molecular landscape of insulin resistance. *Nat Rev Mol Cell Biol* 2021;22:751-71.
6. Tai N, Wong FS, Wen L. The role of gut microbiota in the development of type 1, type 2 diabetes mellitus and obesity. *Rev Endocr Metab Disord* 2015;16:55-65.
7. Ruan W, Engevik MA, Spinler JK, Versalovic J. Healthy human gastrointestinal microbiome: composition and function after a decade of exploration. *Dig Dis Sci* 2020;65:695-705.
8. Jia G, DeMarco VG, Sowers JR. Insulin resistance and hyperinsulinaemia in diabetic cardiomyopathy. *Nat Rev Endocrinol* 2016;12:144-53.
9. DeFronzo RA. Banting lecture. From the triumvirate to the ominous octet: a new paradigm for the treatment of type 2 diabetes mellitus. *Diabetes* 2009;58:773-95.
10. Rodriguez ML, Perez S, Mena-Molla S, Desco MC, Ortega AL. Oxidative stress and microvascular alterations in diabetic retinopathy: future therapies. *Oxid Med Cell Longev* 2019;2019:4940825.
11. Li F, Wang M, Wang J, Li R, Zhang Y. Alterations to the gut microbiota and their correlation with inflammatory factors in chronic kidney disease. *Front Cell Infect Microbiol* 2019;9:206.
12. Li X, Wang Y, Zhou J, Wang Z, Wang Y, Zheng J, et al. Mixed nuts with high nutrient density improve insulin resistance in mice by gut microbiota remodeling. *Food Funct* 2022;13:9904-17.
13. Hao J, Zhang Y, Wu T, Liu R, Sui W, Zhu J, et al. The antidiabetic effects of *Bifidobacterium longum* subsp. *longum* BL21 through regulating gut microbiota structure in type 2 diabetic mice. *Food Funct* 2022;13:9947-58.
14. Zhao D, Zhu H, Gao F, Qian Z, Mao W, Yin Y, et al. Antidiabetic effects of selenium-enriched *Bifidobacterium longum* DD98 in type 2 diabetes model of mice. *Food Funct* 2020;11:6528-41.
15. Butlin M, Tan I, Spronck B, Avolio AP. Measuring arterial stiffness in animal experimental studies. *Arterioscler Thromb Vasc Biol* 2020;40:1068-77.
16. Wang C, Xing C, Li Z, Liu Y, Li Q, Wang Y, et al. Bioinspired therapeutic platform based on extracellular vesicles for prevention of arterial wall remodeling in hypertension. *Bioact Mater* 2021;8:494-504.
17. Chassaing B, Koren O, Goodrich JK, Poole AC, Srinivasan S, Ley RE, et al. Dietary emulsifiers impact the mouse gut microbiota promoting colitis and metabolic syndrome. *Nature* 2015;519:92-6.
18. Cho I, Yamanishi S, Cox L, Methe BA, Zavadil J, Li K, et al. Antibiotics in early life alter the murine colonic microbiome and adiposity. *Nature* 2012;488:621-6.
19. Maddahi A, Edvinsson L. Cerebral ischemia induces microvascular pro-inflammatory cytokine expression via the MEK/ERK pathway. *J Neuroinflammation* 2010;7:14.
20. Hervera A, De Virgiliis F, Palmisano I, Zhou L, Tantardini E, Kong G, et al. Reactive oxygen species regulate axonal regeneration through the release of exosomal NADPH oxidase 2 complexes into injured axons. *Nat Cell Biol* 2018;20:307-19.
21. Zhou J, Zhang L, Zheng B, Zhang L, Qin Y, Zhang X, et al. *Salvia miltiorrhiza* bunge exerts anti-oxidative effects through inhibiting KLF10 expression in vascular smooth muscle cells exposed to high glucose. *J Ethnopharmacol* 2020;262:113208.
22. Hamzah N, Safuan S, Wan Ishak WR. Potential effect of polyphenolic-rich fractions of corn silk on protecting endothelial cells against high glucose damage using in vitro and in vivo approaches. *Molecules* 2021;26:3665.
23. Xu YH, Gao CL, Guo HL, Zhang WQ, Huang W, Tang SS, et al. Sodium butyrate supplementation ameliorates diabetic inflammation in db/db mice. *J Endocrinol* 2018;238:231-44.
24. Yang T, Yang H, Heng C, Wang H, Chen S, Hu Y, et al. Amelioration of non-alcoholic fatty liver disease by sodium butyrate is linked to the modulation of intestinal tight junctions in db/db mice. *Food Funct* 2020;11:10675-89.
25. Mthiyane FT, Dlodla PV, Ziqubu K, Mthembu SX, Muvhulawa N, Hlengwa N, et al. A review on the antidiabetic properties of *Moringa oleifera* extracts: focusing on oxidative stress and inflammation as main therapeutic targets. *Front Pharmacol* 2022;13:940572.
26. Wang H, Lu Y, Yan Y, Tian S, Zheng D, Leng D, et al. Promising treatment for type 2 diabetes: fecal microbiota transplantation reverses insulin resistance and impaired islets. *Front Cell Infect Microbiol* 2020;9:455.
27. Furman D, Campisi J, Verdin E, Carrera-Bastos P, Targ S, Franceschi C, et al. Chronic inflammation in the etiology of disease across the life span. *Nat Med* 2019;25:1822-32.
28. Beckman JA, Paneni F, Cosentino F, Creager MA. Diabetes and vascular disease: pathophysiology, clinical consequences, and medical therapy: part II. *Eur Heart J* 2013;34:2444-52.

29. Machate DJ, Figueiredo PS, Marcelino G, Guimaraes RC, Hi-ane PA, Bogo D, et al. Fatty acid diets: regulation of gut microbiota composition and obesity and its related metabolic dysbiosis. *Int J Mol Sci* 2020;21:4093.
30. Xu J, Lian F, Zhao L, Zhao Y, Chen X, Zhang X, et al. Structural modulation of gut microbiota during alleviation of type 2 diabetes with a Chinese herbal formula. *ISME J* 2015;9:552-62.
31. Avagliano C, De Caro C, Cuozzo M, Liguori FM, La Rana G, Micheli L, et al. *Phaseolus vulgaris* extract ameliorates high-fat diet-induced colonic barrier dysfunction and inflammation in mice by regulating peroxisome proliferator-activated receptor expression and butyrate levels. *Front Pharmacol* 2022;13:930832.
32. Yang YN, Wang QC, Xu W, Yu J, Zhang H, Wu C. The berberine-enriched gut commensal *Blautia producta* ameliorates high-fat diet (HFD)-induced hyperlipidemia and stimulates liver LDLR expression. *Biomed Pharmacother* 2022;155:113749.
33. Wang FY, Liu JM, Luo HH, Liu AH, Jiang Y. Potential protective effects of *Clostridium butyricum* on experimental gastric ulcers in mice. *World J Gastroenterol* 2015;21:8340-51.
34. Liu J, Fu Y, Zhang H, Wang J, Zhu J, Wang Y, et al. The hepatoprotective effect of the probiotic *Clostridium butyricum* against carbon tetrachloride-induced acute liver damage in mice. *Food Funct* 2017;8:4042-52.
35. Jia L, Li D, Feng N, Shamoon M, Sun Z, Ding L, et al. Anti-diabetic effects of *Clostridium butyricum* CGMCC0313.1 through promoting the growth of gut butyrate-producing bacteria in type 2 diabetic mice. *Sci Rep* 2017;7:7046.
36. Jia L, Shan K, Pan LL, Feng N, Lv Z, Sun Y, et al. *Clostridium butyricum* CGMCC0313.1 protects against autoimmune diabetes by modulating intestinal immune homeostasis and inducing pancreatic regulatory T cells. *Front Immunol* 2017;8:1345.
37. Malik A, Morya RK, Saha S, Singh PK, Bhadada SK, Rana SV. Oxidative stress and inflammatory markers in type 2 diabetic patients. *Eur J Clin Invest* 2020;50:e13238.
38. Li H, Shi Y, Wang X, Li P, Zhang S, Wu T, et al. Piceatannol alleviates inflammation and oxidative stress via modulation of the Nrf2/HO-1 and NF- $\kappa$ B pathways in diabetic cardiomyopathy. *Chem Biol Interact* 2019;310:108754.
39. Ichikawa T, Li J, Meyer CJ, Janicki JS, Hannink M, Cui T. Dihydro-CDDO-trifluoroethyl amide (dh404), a novel Nrf2 activator, suppresses oxidative stress in cardiomyocytes. *PLoS One* 2009;4:e8391.
40. Nguyen T, Sherratt PJ, Pickett CB. Regulatory mechanisms controlling gene expression mediated by the antioxidant response element. *Annu Rev Pharmacol Toxicol* 2003;43:233-60.
41. Uruno A, Furusawa Y, Yagishita Y, Fukutomi T, Muramatsu H, Negishi T, et al. The Keap1-Nrf2 system prevents onset of diabetes mellitus. *Mol Cell Biol* 2013;33:2996-3010.
42. Di Marco E, Jha JC, Sharma A, Wilkinson-Berka JL, Jandeleit-Dahm KA, de Haan JB. Are reactive oxygen species still the basis for diabetic complications? *Clin Sci (Lond)* 2015;129:199-216.